청정/대체에너지기술

광전기화학 전지를 위한 질소 도핑된 WO_3 박막의 후열처리 효과

안광순*

영남대학교 디스플레이화학공학부
712-749 경북 경산시 대동 214-1

(2009년 8월 14일 접수; 2009년 8월 26일 수정본 접수; 2009년 8월 27일 채택)

Post-annealing Effect of N-incorporated WO_3 Films for Photoelectrochemical Cells

Kwang-Soon Ahn*

School of Display and Chemical Engineering, Yeungnam University
214-1 Dae-dong, Gyeongsan, Gyeongbuk 712-749, Korea

(Received for review August 14, 2009; Revision received August 26, 2009; Accepted August 27, 2009))

요 약

질소 도핑된 WO_3 (WO_3:N) 막을 반응성 RF 마그네트론 스퍼터링을 이용하여 상온에서 증착한 다음, 300°C에서부터 500°C의 온도 구간에서 후열처리(post-annealing)하였다. WO_3 내 질소 음이온은 O 2p valence state와의 mixing effect에 의해 광학적 밴드갭을 줄임으로써 장파장 영역의 빛을 흡수할 수 있었다. 더욱이 350°C 이상의 후열처리에 의해 WO_3:N의 결정성이 크게 향상됨을 발견하였으며, 동일 온도에서 열처리된 순수한 WO_3 막보다 광전기화학 특성이 훨씬 우수한 셀 성능을 가짐을 알 수 있었다.

주제어: 질소 도핑된 WO_3, 광전기화학적, 후열처리, 결정성, 밴드갭

Abstract : N-incorporated WO_3 (WO_3:N) films were synthesized using a reactive RF magnetron sputtering on unheated substrate and then post-annealed at different temperatures from 300 to 500°C in air. The N anion narrowed optical band gap, due to its mixing effect with the O 2p valence states. Furthermore, it was found that the crystallinity of the WO_3:N films was significantly improved by the post-annealing at 350°C and higher. As a result, the WO_3:N films exhibited much better photoelectrochemical performance, compared with pure WO_3 films post-annealed at the same temperature.

Keywords: N-incorporated WO_3, Photoelectrochemical, Post-annealing, Crystallinity, Band gap

1. Introduction

Photoelectrochemical cell (PEC) systems are promising methods for producing H_2 gas in an aqueous solution by solar energy[1-7]. To improve photoelectrochemical properties, the following photoelectrode properties are desirable: (1) a photoelectrode that has high contact area with the electrolyte to increase the interfacial reaction site, (2) a photoelectrode that has a narrow bandgap to use visible-light energy, and (3) a photoelectrode that has a good crystallinity to reduce the recombination rate of photogenerated electrons and holes. WO_3 has been extensively studied in many other technological areas such as electrochromism[8-10], photocatalysis[11], and gas sensors[12], due to their nontoxic, stable, and native n-type semiconductor properties. WO_3 is also one of the few inexpensive semiconductors resistant against photocorrosion in

* E-mail: kstheory@ynu.ac.kr

an acidic aqueous solution, whose promising utilities in the PEC systems were demonstrated by Miller et al.[13,14] Recently, WO_3 electrodes with nanoporous and nanostructured morphologies have been studied to improve photoelectrochemical properties [15-17] pertaining to the above (1). However, energy band gaps, reported from 3.4 to 2.6 eV with variations in crystallinity, only allow the light absorption in the near ultraviolet and blue wavelength region. Thus, the band gap modification would be necessary to use sunlight more efficiently.

Impurity doping in the photoactive metal oxides has been known to shift light absorption to longer wavelengths. Asahi et al.[2] reported that nitrogen anion doping of TiO_2 was one of the most effective ways of increasing photo-catalytic activity, because its p-states mix with O 2p-valence band, resulting in the band gap narrowing. In a similar manner, N incorporation into WO_3 was recently reported by Paluselli et al.[18], whose band gap could be successfully narrowed down up to 2.2 eV with increasing the concentration of nitrogen. However, despite its effective bandgap narrowing, few results have been, to date, reported relating to the photoelectrochemical responses, due to its inferior crystallinity. Therefore, a good crystallinity is also required for the highly improved photoelectrochemical properties, together with better light absorption in the long wavelength region.

In this article, the N-incorporated WO_3 (WO_3:N) film was deposited on the substrates, which is not heated, using a reactive RF magnetron sputtering, followed by post-annealing in air at temperatures ranging from 300 to 500°C. Structural, optical, and photoelectrochemical properties of these films were then investigated as a function of increased annealing temperature and compared to those of pure WO_3 films without N incorporation. Our data and analyses report that post-annealing of the WO_3:N films at temperatures higher than 350°C greatly enhance the crystallinity as well as the band gap narrowing effect of N, compared to the pure WO_3 films, resulting in superior photoelectrochemical responses. We also expect that it should prompt developing other technologies such as the electrochromic devices, photocatalysts, and gas sensors.

2. Experimental

WO_3:N films were deposited on the non-heated substrates using a reactive RF magnetron sputtering system followed by post-annealing at different temperatures from 300 to 500°C in air for 5 hr. Conducting transparent FTO (20–23 Ω/sq.)-coated glass was used as the substrate to allow PEC measurements. The distance between the W metal target and substrate was about 10 cm. The base pressure was below 1×10^{-6} torr and the working pressure was 8.8×10^{-3} torr. The chamber was mixed with N_2 and O_2 flowing at an oxygen gas ratio, $O_2/(N_2+O_2)$ = 3.3%. This low O_2 gas flow ratio was required because of its high chemical activity. Prior to sputtering, a pre-sputtering cleaning was performed for 30 min to eliminate possible contaminants from the target. Sputtering was then conducted at a RF power of 150 W. For comparison, a pure WO_3 film was deposited at a RF power of 150 W in pure O_2 gas environment. All the sputtered samples were controlled to have same film thickness of 1 μm as measured by stylus profilometry.

The characterization of structure and crystallinity were performed by X-ray diffraction (XRD) measurements, using an X-ray diffractometer (XGEN-4000, SCINTAG Inc.), operated with a Cu Kα radiation source at 45 kV and 37 mA. The N concentration in the WO_3:N films was evaluated by X-ray photoelectron spectroscopy (XPS). The UV-Vis absorption spectra of the samples were measured by n&k analyzer 1280 (n&k Technology, Inc.) to investigate the optical properties.

Photoelectrochemical measurements were performed in a three-electrode cell with a flat quartz-glass window to facilitate illumination to the photoelectrode surface. The sputter-deposited films were used as the working electrodes. A strip of Pt mesh and an Ag/AgCl electrode were used as the counter and reference electrodes, respectively. A 1-M H_2SO_4 aqueous solution was used as the electrolyte for the PEC measurements. The photoelectrochemical response was measured using a fiber optic illuminator (150 W tungsten-halogen lamp) with a UV/IR and combined UV/IR and green filter. The light intensity was measured by a photodiode power meter, in which the total light intensity with the UV/IR filter was fixed at 125 mW/cm^2. The photoelectrochemical response data under light on/off illumination were also measured to confirm the photoresponse of the films during the potential sweep (scan rate: 5 mV/s).

3. Results and Discussions

Figures 1(a) and (b) show X-ray diffraction curves for the WO_3 and WO_3:N films, respectively, annealed at different temperatures. Here, numbers of the samples in Y-axis indicate substrate, as-grown film, and 300, 350, 400, and 500°C-annealed

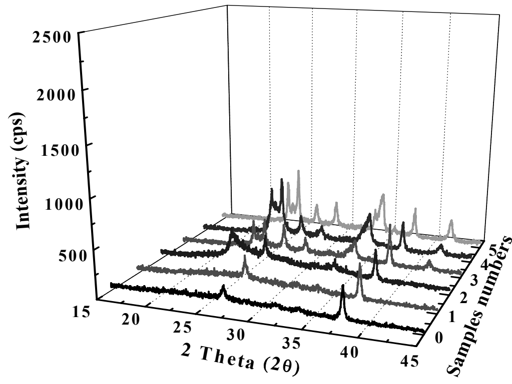

(a)

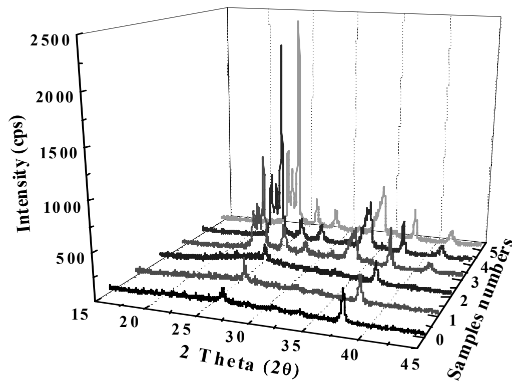

(b)

Figure 1. X-ray diffraction data for the (a) WO_3 and (b) WO_3:N films annealed at different temperatures from 300 to 500℃ in air.

films for (0) to (5), respectively. Both of the unheated as-grown WO_3 and WO_3:N films exhibited amorphous structures and the crystallinity of the film could be gradually improved with increasing the annealing temperature. Figure 2 showed the expanded intensity scale for substrate and the WO_3 and WO_3:N annealed at 350°C. It clearly shows that both of the annealed WO_3 and WO_3:N films display a monoclinic, polycrystalline structure with a main peak at 24.4° corresponding to a (200) plane. Crystallite sizes of the WO_3:N films estimated according to the Debye-Sherrer equation were compared to those of the WO_3 films, as shown in Figure 3. The WO_3:N films annealed at 350°C or higher exhibited much superior crystallinity than the pure WO_3 films, which may be related to the existence of N atoms in the WO_3:N film. Figure 3 shows the N concentrations of at% with the annealing temperature for the WO_3:N films, as measured by X-ray photoelectron spectroscopy. The as-grown WO_3:N film was highly incorporated by the N concentration of about 7.6 at%.

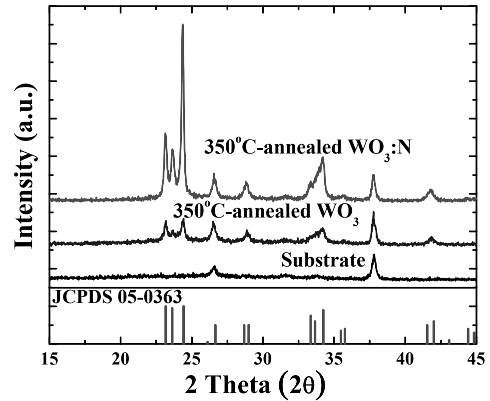

Figure 2. The expended intensity scale for the WO_3 and WO_3:N films annealed at 350℃.

With increasing in the annealing temperature, the N concentration rapidly decreased up to 350°C and then maintained in low N concentration of about 1.5 at% without decrease of the N concentration, indicating that the N atoms were diffused outside the film during the post-annealing and the N solubility limit of about 1.5 at% remained in the film. From Figures 1(a) and (b), the WO_3:N film annealed at 300°C exhibited less crystallinity than the WO_3 film at 300°C. It is generally known that excess dopant incorporation can deteriorate the film crystallinity[18-20]. Therefore, inferior crystallinity of the film can be attributed to the existence of still high N incorporation level, as shown in Figure 3, which is in a good agreement with the result reported by Paluselli et al.[18]. On the other hand, greatly enhanced crystallinity of the WO_3:N films annealed at 350°C and higher may be due to the moderate amount of N concentration. Similar phenomena have

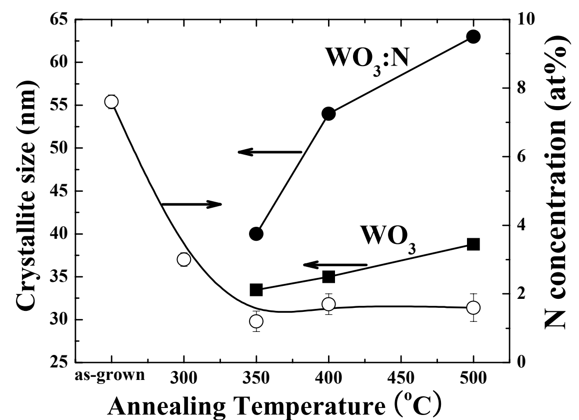

Figure 3. Crystallite sizes of the annealed WO_3 and WO_3:N films and the N concentrations for the WO_3:N films as a function of the annealing temperature.

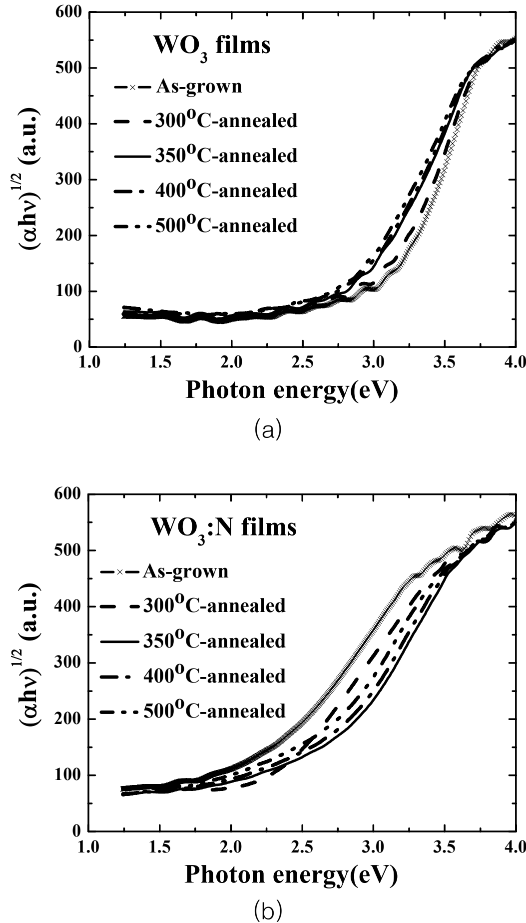

Figure 4. Indirect-transition absorption coefficients for the (a) WO_3 and (b) WO_3:N films with the different annealing temperatures.

been observed in the Cu-doped, Mn-doped and Bi-doped ZnO films[19,21,22]. They reported that the moderate amount of dopant can reduce activation energy of grain growth or share the oxygen atoms with the metal atoms, leading to the improved crystallinity. Our group previously reported[23] that, when the ZnO is deposited under the mixed sputtering ambient with Ar and N_2 at high temperature region, the nitrogen modifies the growth mode and results in the significantly enhanced crystallinity, as compared with the films deposited under pure Ar ambient. More detailed studies of the N effect on the crystallinity are underway.

Figures 4(a) and (b) show indirect-transition absorption coefficient curves for the WO_3 and WO_3:N films, respectively, with the different annealing temperatures. An indirect optical band gap can be described by the following Eq. 1[18];

$$(\alpha h\nu)^{1/2} = \beta(h\nu - E_g) \tag{1}$$

where $h\nu$ is photon energy, E_g is an optical bandgap, and β is the edge width. The absorption coefficient α was calculated by the following Eq. 2[18]:

$$\alpha = -\frac{1}{d}\ln\left(\frac{T}{1-R}\right) \tag{2}$$

where d, R, and T are the film thickness, the measured reflectance and transmittance, respectively. The indirect optical band gaps of the films were determined by extrapolating the linear portion of each curve in Figures 4(a) and (b) to $(\alpha h\nu)^{1/2} = 0$, as shown in Figure 5. The amorphous as-grown WO_3 film had larger band gap (3.1 eV) than other annealed WO_3 films, due to band gap widening via the quantum confinement effect in semiconductor clusters[18,24,25]. The band gap of the pure WO_3 films gradually decreased with an increase of the annealing temperature, which is in good agreement with results reported by other groups[24,25]. The as-grown WO_3:N film exhibited significantly low band gap less than 2 eV, due to highly incorporated N. However, as increasing the annealing temperature up to 350°C, the band gap of the WO_3:N films increased due to the rapidly reduced N concentration, despite superior crystallinity. Thereafter, the bandgap of the WO_3:N films gradually decreased from 350 to 500°C, because the crystallinity is enhanced whereas the N concentration is almost constant, as shown in Figures 1(b) and 3. It is worth noting that even the 350°C-annealed WO_3:N film exhibited much lower band gap than the 500°C-annealed WO_3 film, indicating that this considerable band gap reduction is mainly owing to the band gap narrowing by the N doping, because the 350°C-annealed

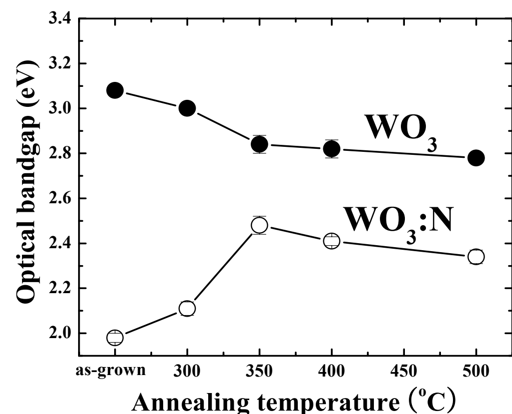

Figure 5. Estimated optical band gaps of the WO_3 and WO_3:N films as a function of annealing temperature.

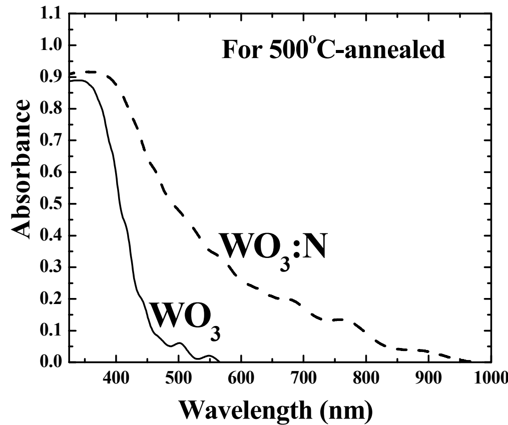

Figure 6. Absorption spectra of the 500℃-annealed WO_3 and WO_3: N films.

WO_3:N film has slightly better crystallinity than the 500°C-annealed WO_3. Figure 6 shows typical optical- absorption spectra of the WO_3 and WO_3:N films, respectively, annealed at 500°C. To eliminate the effect from the FTO substrate, the absorbance was calculated by $A = 1 - R(film) - T(film) / T(substrate)$ [20,26]. The 500°C-annealed WO_3:N film exhibited an absorption tail in the long wavelength region as well as the red-shift of the absorption edge, compared to the WO_3 annealed at 500°C. Photoelectrochemical responses of all of WO_3:N films in our experiments exhibited n-type photoresponses, which will be discussed later. It indicates that additional n-type donor states such as oxygen vacancy or N-induced new states near the conduction band were simultaneously produced when the N is incorporated. Therefore, the absorption tails in the long wavelength region of the WO_3:N films can be attributed to the generation of additional donor states such as the oxygen vacancy or the N-induced new states near the conduction band.

Figure 7 shows photocurrent-voltage curves of the WO_3 and WO_3:N films, respectively, annealed at 500°C under light illumination with an UV/IR filter. Only freshly prepared samples were used for this photoresponse experiment. The 500°C-annealed WO_3:N film exhibited anodic photoresponse. All of the other WO_3:N films also showed n-type anodic photoresponses (not shown here), although substitutional N dopants occupied at O sites act as p-type acceptors. Therefore, it indicates that the additional n-type donor states were simultaneously generated when the N is incorporated, which is corresponding well to the absorption spectra in Figure 6. The 500°C-annealed WO_3:N film exhibited superior photoelectrochemical property than the WO_3 annealed at 500°C. To confirm whether the photoresponse of the 500°C-annealed WO_3:N film was generated by only absorbed photons without any dark current component, the photoelectrochemical response under light on/off illumination was measured and shown in Figure 7. The currents under light on and off conditions are the same as the photocurrent under illumination and the dark current, respectively, indicating that the photocurrent of the 500°C-annealed WO_3:N film is generated only by absorbed photons under illumination without the contribution of the dark current.

Figure 8 shows the photocurrents measured at 1.6 V as a function of the annealing temperature for the WO_3 and WO_3:N films. The as-grown and 300°C-annealed WO_3 and WO_3:N films hardly exhibit the photocurrents. Thereafter, the photocurrent increase with increasing the annealing temperature above 350°C for both of the WO_3 and WO_3:N films. These trends agree well with the results in Figure 1. The enhanced crystallinity reduces the recombination rate for the

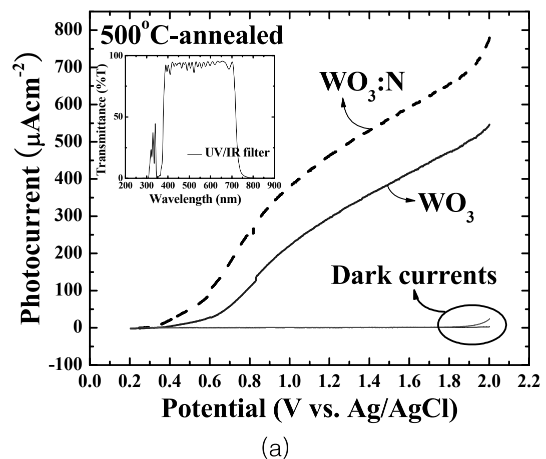

(a)

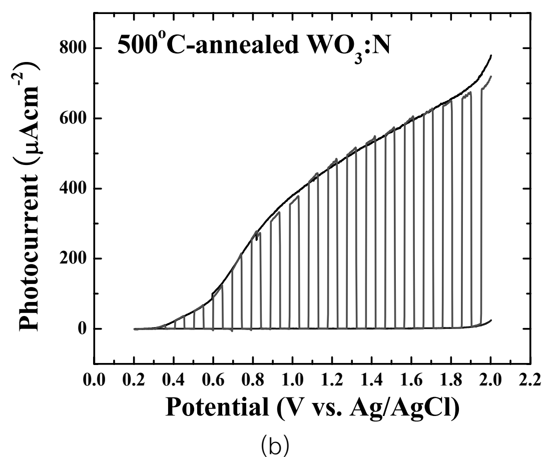

(b)

Figure 7. Photocurrent-voltage curves (1 M H_2SO_4 aq. sol. electrolyte and 5 mV/s of scan rate): (a) the 500℃-annealed WO_3 and WO_3:N films under illumination with an UV/IR filter, (b) the 500℃-annealed WO_3: N films under light on/off illumination.

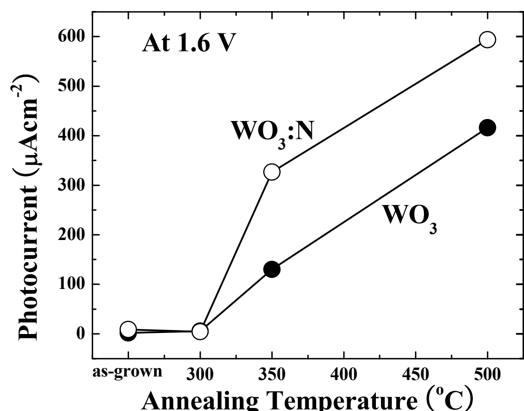

Figure 8. Photocurrents measured at 1.6 V as a function of the annealing temperature for the WO_3 and WO_3:N films.

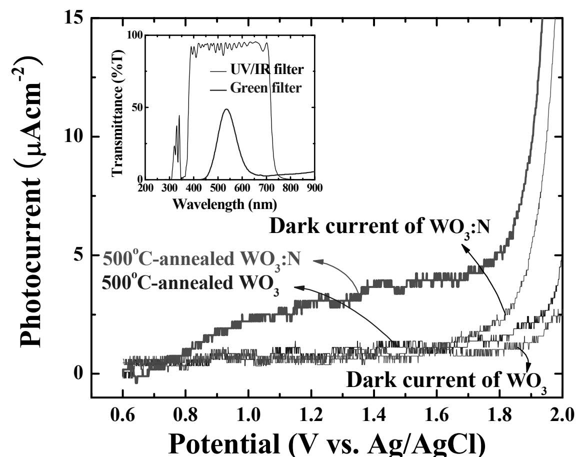

Figure 9. Photocurrent-voltage curves of the 500℃-annealed WO_3 and WO_3:N films under light illumination using both the UV/IR and green filters.

photogenerated electrons and holes, resulting in the improved photoelectrochemical property. Figure 8 also shows that the WO_3:N films annealed at 350°C and higher exhibited superior photoresponses than those of the annealed WO_3 films. It is attributed to their better light absorption in the longer wavelengths as well as their excellent crystallinity. In order to investigate the photoelectrochemical response in the long wavelength region, a green color filter was used in combination with the UV/IR filter. Figure 9 shows photocurrent- voltage curves of the WO_3 and WO_3:N films annealed at 500°C under light illumination with the combined filter. The 500°C-annealed WO_3 scarcely exhibit photoresponse, compared to the dark current, which corresponds well to the optical absorption result in Figure 6. On the other hand, the WO_3:N film annealed at 500°C exhibited the photoelectrochemical response in this long wavelength region. It indicates that, in the case of WO_3:N, electron-hole pairs could be generated by light absorption in the longer wavelengths, leading to the photoactive response in the longer wavelength region. It is interesting to note that the photoelectrochemical property of the WO_3:N films was not improved in proportion to the dramatically enhanced crystallinity as shown in Figure 1. It indicates that some other recombination centers exist in the WO_3:N films. From the analysis of Figure 6 and Figure 7, the WO_3:N films most likely contained the additional n-type donor states such as the oxygen vacancy or the N-induced new states near the conduction band, leading to the recombination centers; the photogenerated electrons and holes are trapped by these additional donor states, limiting photoelectrochemical response. Nevertheless, the crystalline, N-incorporated WO_3 films exhibited excellent photoelectrochemical responses, owing to the greatly enhanced crystallinity and better light absorption generated from a bandgap narrowing.

4. Conclusions

In summary, the crystalline, N-incorporated WO_3 films have been successfully fabricated by the reactive RF magnetron sputtering followed by the post-annealing process in air. The crystallinity of the WO_3:N films could be dramatically enhanced by the post-annealing of above 350°C when compared to those of the WO_3 films. The N concentration decreased and was then constant in the temperature more than 350°C, whereas the crystallinity was significantly improved as the annealing temperature increased. As a result, the bandgaps of the annealed WO_3:N films were narrowed below 2.5 eV due to the N 2p states mixed with the O 2p valence-band states as well as the enhanced crystallinity. However, the N-incorporation into the WO_3 created, at a same time, additional n-type donor states such as the oxygen vacancy or the N-induced new states near the conduction band that trap the photogenerated carriers. Nevertheless, the WO_3:N films annealed at 350°C and higher exhibited much better photoelectrochemical responses than the annealed WO_3 films. It is due to the greatly enhanced crystallinity and better light absorption in the longer wavelength region. Although more detailed studies for the WO_3:N films are required, these results will significantly impact current PEC technologies and have promising implications for the development of electrochromic

devices, photocatalysts, and gas sensors.

Acknowledgement

This research was supported by the Yeungnam University research grant (209-A-054-030) for the PEC application.

References

1. Fujishima, A., and Honda, K., "Electrochemical Photolysis of Water at a Semiconductor Electrode," *Nature*, **238**, 37-38 (1972).
2. Asahi, R., Morikawa, T., Ohwaki, T., Aoki, K., and Taga, Y., "Visible-Light Photocatalysis in Nitrogen-Doped Titanium Oxides," *Science*, **293**, 269-271 (2001).
3. Khaselev, O., and Turner, J. A., "A Monolithic Photovoltaic-Photoelectrochemical Device for Hydrogen Production via Water Splitting," *Science*, **280**, 425-427 (1998).
4. López, C. M., and Choi, K. S., "Enhancement of Electrochemical and Photoelectrochemical Properties of Fibrous Zn and ZnO Electrodes," *Chem. Commun.,* 3328-3330 (**2005**).
5. Ghicov, A., Tsuchiya, H., Macak, J. M., and Schmuki, P., "Annealing Effects on the Photoresponse of TiO_2 Nanotubes," *Phys. Status. Solidi. A*, **203**, R28-R30 (2006).
6. Mor, G. K., Shankar, K., Paulose, M., Varghese, O. K., and Grimes, C. A., "Enhanced Photocleavage of Water Using Titania Nanotube Arrays," *Nano Lett*., **5**, 191-195 (2005).
7. O'Regan, B., and Grätzel, M., "A Low-cost, High-efficiency Solar Cell based on Dye-Sensitized Colloidal TiO_2 Films," *Nature*, **353**, 737-740 (**1991)**.
8. Lee, S.-H., Deshpande, R., Parilla, P. A., Jones, K. M., To, B., Mahan, A. H., and Dillon, A. C., "Crystalline WO_3 Nanoparticles for Highly Improved Electrochromic Applications," *Adv. Mater.*, **18**, 763-766 (2006).
9. Lee, S.-H., Cheong, H. M., Tracy, C. E., Mascarenhas, A., Pitts, J. R., Jorgensen, G., and Deb, S. K., "Alternating Current Impedance and Raman Spectroscopic Study on Electrochromic *a*-WO_3 Films," *Appl. Phys. Lett*., **76**, 3908-3910 (2000).
10. Wang, Y., and Herron, N., "Nanometer-Sized Semiconductor Clusters: Materials Synthesis, Quantum Size Effects, and Photophysical Properties," *J. Chem. Phys*., **95**, 525-532 (1991).
11. Bosch, H., and Janssen, F., "Formation and Control of Nitrogen Oxides," *Catal. Today*, **2**, 369-379 (1988).
12. Tao, W. H., and Tsai, C. H., "H_2S Sensing Properties of Noble Metal Doped WO_3 Thin Film Sensor Fabricated by Micromachining," *Sensor. Actuat. B-Chem*., **81**, 237-247 (2002).
13. Miller, E. L., Paluselli, D., Marsen, B., and Rocheleau, R. E., "Development of Reactively Sputtered Metal Oxide Films for Hydrogen-Producing Hybrid Multijunction Photoelectrodes," *Sol. Energ. Mat. Sol. C.*, **88**, 131-144 (2005).
14. Miller, E. L., Marsen, B., Paluselli, D., and Rocheleau, R., "Optimization of Hybrid Photoelectrodes for Solar Water-Splitting," *Electrochem. Solid St.*, **8**, A247-A249 (2005).
15. Santato, C., Ulmann, M., and Augustynski, J., "Photoelectrochemical Properties of Nanostructured Tungsten Trioxide Films," *J. Phys. Chem. B*, **105**, 936-940 (2001).
16. Berger, S., Tsuchiya, H., Ghicov, A., and Schmuki, P., "High Photocurrent Conversion Efficiency in Self-Organized Porous WO_3," *Appl. Phys. Lett*., **88**, 203119 (2006).
17. de Tacconi, N. R., Chenthamarakshan, C. R., Yogeeswaran, G., Watcharenwrong, A., de Zoysa, R. S., Basit, N. A., and Rajeshwar, K., "Nanoporous TiO_2 and WO_3 Films by Anodization of Titanium and Tungsten Substrates: Influence of Process Variables on Morphology and Photoelectrochemical Response," *J. Phys. Chem. B*, **110**, 25347-25355 (2006).
18. Paluselli, D., Marsen, B., Miller, E.L., and Rocheleau, R. E., "Nitrogen Doping of Reactively Sputtered Tungsten Oxide Films," *Electrochem. Solid St.***, 8**, G301-G303 (2005).
19. Wang, X. B., Li, D. M., Zeng, F., and Pan, F., "Microstructure and Properties of Cu-Doped ZnO Films Prepared by dc Reactive Magnetron Sputtering," *J. Phys. D Appl. Phys.*, **38**, 4104-4108 (2005).
20. Ahn, K.-S., Yan, Y, and Al-Jassim, M., "Band Gap Narrowing of ZnO:N Films by Varying rf Sputtering Power in O_2/N_2 Mixtures," *J. Vac. Sci. Technol. B* **25**, L23-L26 (2007).
21. Han, J., Mantas, P. Q., and Senos, A. M. R., "Grain Growth in Mn-Doped ZnO," *J. Eur. Ceram. Soc.*, **20**, 2753-2758 (2000).
22. Senda, T., and Bradt, R. C., "Grain Growth in Sintered

ZnO and ZnO-Bi_2O_3 Ceramics," *J. Am. Ceram. Soc.*, **73**, 106-114 (1990).

23. Ahn, K.-S., Shet, S., Deutsch, T., Jiang, C.-S., Yan, Y., Al-Jassim, M., and Turner, J., "Enhanced of Photoelectrochemical Response by Aligned Nanorods in ZnO Thin Films," *J. Power Sources*, **176**, 387-392 (2008).
24. Granqvist, C. G., Handbook of Inorganic Electrochromic Materials, Elsevier, New York, 1995.
25. Ahn, K.-S., Lee, S.-H., Dillon, A. C., Tracy, C. E., and Pitts, R., "The Effect of Thermal Annealing on Photoelectrochemical Responses of WO_3 Thin Films," *J. Appl. Phys*. **101,** 093524 (2007).
26. Keis, K., Vayssieres, L., Rensmo, H., Lindquist, S. E., and Hagfeldt, A., "Photoelectrochemical Properties of Nano- to Microstructured ZnO Electrodes," *J. Electrochem. Soc*., **148**, A149-A155 (2001).